

ReFLEX: Length-Generalizable CSI Denoising for MIMO-OFDM via Relative-Frequency Bias

Zhibin Zhang, Robert N. Potekhin, Ziwei Wan, *Member, IEEE*, Vladimir Lyashev, *Senior Member, IEEE*, and Zhen Gao, *Senior Member, IEEE*

Abstract—This letter studies CSI denoising for MIMO-OFDM with variable NR resource block (RB) allocations. ReFLEX is a length-generalizable Transformer whose frequency attention uses a relative-frequency position bias (RFPB) generated from subcarrier offsets. A single checkpoint handles unseen RB lengths and can be applied to sparse DM-RS observations in the tested RB5/RB10 PUSCH setup without retraining. In a 3GPP TR 38.901 UMa NLOS channel, ReFLEX achieves about -9.6 dB NMSE on unseen RB lengths. In NR PUSCH/UL-SCH simulations, ReFLEX denoising followed by time-frequency interpolation reduces the 10% BLER threshold by about 2–3 dB.

Index Terms—MIMO-OFDM, CSI denoising, DM-RS, length generalization, relative-frequency bias.

I. INTRODUCTION

MIMO-OFDM receivers require accurate channel state information (CSI) for equalization, detection, and decoding. Classical denoising and refinement methods include DFT-based truncation and LMMSE filtering. The performance of these methods depends on selecting a delay window as well as having knowledge of the channel covariance and noise variance [1], [2]. Neural CSI estimators based on convolutional, residual, attention-based, and generative architectures have also been studied [3]–[6]. Prior massive-MIMO CSI denoising work further showed that vector autoregression and tensor DnCNN models can improve noisy SRS-based channel estimates when combined with beam-delay-sparse representations [7].

In the reported setups, the closest related neural estimators remain tied to a fixed grid or preprocessing chain. Channelformer [4] applies self-attention to LS-based OFDM channel estimation and studies online adaptation, but its reported NR setup fixes $N_f = 72$ subcarriers and the authors note that retraining is needed for significant changes such as the number of subcarriers. The beam-delay tensor DnCNN in [7] targets SRS-based TDD massive-MIMO denoising and reports downlink SINR-oriented results. It first maps antenna-frequency CSI to a sparse beam-delay tensor using antenna-to-beam and frequency-to-delay DFT operations, applies a three-dimensional CNN denoiser, and then transforms the output back. This pipeline exploits sparsity, but it adds transform steps

Zhibin Zhang, Robert N. Potekhin, and Vladimir Lyashev are with the Moscow Institute of Physics and Technology (State University), Moscow, Russia (e-mails: zhibin@phystech.edu; potekhin.rn@phystech.edu; lyashev.va@mipt.ru).

Ziwei Wan is with the Yangtze Delta Region Academy, Beijing Institute of Technology (Jiaxing), Jiaxing 314019, China (e-mail: ziweiwan@bit.edu.cn).

Zhen Gao is with the School of Interdisciplinary Science, Beijing Institute of Technology, Beijing 100081, China (e-mail: gaozhen16@bit.edu.cn).

and was evaluated under fixed bandwidth, subcarrier spacing, and SRS-comb settings. Swin/cGAN-based estimation and diffusion inpainting techniques can exploit multi-slot pilot structures or handle noisy, sparse observations under varying pilot patterns and noise levels [5], [6]. However, these forms of robustness alone do not demonstrate that a single checkpoint can process RB lengths that were absent during training.

This fixed-grid dependence matters in NR uplink scheduling, where RB allocations vary with traffic and bandwidth constraints [8]. Separate checkpoints for different RB lengths and SNR settings increase model-management cost, whereas fixed-length implementations generally cannot directly process untrained RB lengths. ReFLEX avoids relying on fixed frequency-position encoding tables by generating the attention bias from pairwise subcarrier offsets. This allows the same parameter set to be evaluated on the offset matrix induced by a new RB allocation.

We focus on RB-length generalization for CSI denoising and refinement from noisy channel estimates under fixed subcarrier spacing. The model operates on observed subcarrier positions (i.e., frequency-domain samples), which may be a dense observation set containing all allocated subcarriers or a sparse DM-RS observation set. When a receiver requires CSI on the data grid, the denoised sparse estimates are linearly interpolated across time and frequency.

We propose ReFLEX, a *relative-frequency length-extensible* Transformer. ReFLEX preserves the frequency, polarization, and array dimensions of MIMO-OFDM CSI and applies axial attention along those dimensions. Its key mechanism is a relative-frequency position bias: the frequency-attention bias is generated as a continuous function of the relative subcarrier offsets rather than learned as a fixed absolute-position table. Under wide-sense stationary channel models, frequency correlation is more naturally tied to frequency separation than to an absolute subcarrier index. This structure allows the same RFPB parameters to generate a bias matrix for a new RB length or sparse observation set from the corresponding pairwise offsets.

Our contributions are: (i) we formulate and evaluate RB-length generalization for CSI denoising with a single parameter set; (ii) we propose ReFLEX combining tensor-preserving axial attention with continuous RFPB for variable RB lengths; and (iii) we report NMSE and BLER results on 3GPP UMa NLOS and NR PUSCH/UL-SCH scenarios (RB5/RB10).

II. SYSTEM MODEL AND PROBLEM FORMULATION

We consider per-user uplink CSI denoising and refinement on observed subcarrier positions. For an allocation of R

resource blocks (RBs) with $N_{sc} = 12R$ subcarriers, let $\mathcal{S}_R = \{s_1, \dots, s_{M_R}\} \subseteq \{1, \dots, N_{sc}\}$ denote the observed subcarriers used as model input. Dense NMSE experiments use $M_R = N_{sc}$, whereas a sparse DM-RS input has $M_R < N_{sc}$. For compact notation, $\mathbf{H}_R \in \mathbb{C}^{M_R \times A \times P}$ denotes the normalized frequency-domain channel restricted to \mathcal{S}_R . Here $A = 64$ is the number of elements in the 8×8 base-station antenna array and $P = 2$ denotes dual polarization, yielding $AP = 128$ receive ports. The channel is normalized by sample power so that errors remain comparable across RB lengths and channel realizations.

Let $\tilde{\mathbf{H}}_R$ denote the normalized noisy input at the same observation locations:

$$\tilde{\mathbf{H}}_R = \mathbf{H}_R + \mathbf{E}_R, \quad (1)$$

where $\mathbf{E}_R \sim \mathcal{CN}(\mathbf{0}, \sigma^2 \mathbf{I})$ models independent LS noise at the observation points. The denoiser estimates \mathbf{H}_R on \mathcal{S}_R . When link-level detection requires CSI on PUSCH data resource elements, the denoised sparse estimates are linearly interpolated over time and frequency. The model input stacks the real and imaginary parts of $\tilde{\mathbf{H}}_R$ as

$$\mathbf{X}_R \in \mathbb{R}^{P \times M_R \times 2 \times 8 \times 8}, \quad (2)$$

preserving the frequency, polarization, and two-dimensional array structure.

The model is trained on the RB-length set $\mathcal{R}_{tr} = \{2, 4, 6\}$, corresponding to 24, 48, and 72 subcarriers respectively. It is tested on $\mathcal{R}_{te} = \{2, 3, 4, 5, 6, 8, 10\}$, where the unseen RB-length subset is $\mathcal{R}_{un} = \mathcal{R}_{te} \setminus \mathcal{R}_{tr} = \{3, 5, 8, 10\}$. A single parameter set is used for all test RB lengths and for the sparse DM-RS BLER evaluation.

Let γ denote the sample-level SNR. The estimator is

$$\hat{\mathbf{H}}_R = f_{\theta}(\tilde{\mathbf{H}}_R, \gamma), \quad (3)$$

where θ is shared across RB lengths. The RB length R appears only through the observed subcarrier positions \mathcal{S}_R and does not require a separate branch. During training, the model uses dense subcarrier observations with $\mathcal{S}_R = \{1, \dots, N_{sc}\}$. For RB5/RB10 PUSCH, the dense-trained checkpoint is directly evaluated on sparse DM-RS observations without additional retraining. The loss is the sample-power-normalized mean-square error:

$$\mathcal{L}(\theta) = \mathbb{E}_{R, \gamma} \left[\frac{\left\| f_{\theta}(\tilde{\mathbf{H}}_R, \gamma) - \mathbf{H}_R \right\|_F^2}{\left\| \mathbf{H}_R \right\|_F^2} \right]. \quad (4)$$

CSI denoising performance is measured by

$$\text{NMSE} = \mathbb{E} \left[\frac{\left\| \hat{\mathbf{H}}_R - \mathbf{H}_R \right\|_F^2}{\left\| \mathbf{H}_R \right\|_F^2} \right], \quad (5)$$

reported as $10 \log_{10}(\text{NMSE})$. Link-level impact is measured by block error rate (BLER) in a common PUSCH receiver chain where only the CSI estimate supplied to the equalizer is changed.

III. PROPOSED REFLEX

ReFLEX is designed for single-checkpoint CSI denoising with variable frequency-domain lengths. As shown in Fig. 1, it combines a tensor-preserving input and reconstruction path, axial attention over frequency, polarization, and spatial dimensions, and RFPB for RB-length generalization. All trainable parameters are shared across RB lengths; only the relative-offset matrix changes for a new RB length or sparse observation set.

A. Overall Architecture

For an input with M_R observed subcarrier positions, the noisy CSI is arranged as

$$\mathbf{X}_R \in \mathbb{R}^{B \times P \times M_R \times 2 \times H \times V}, \quad (6)$$

where B is the batch size, $P = 2$, $H \times V$ is the two-dimensional base-station antenna-array grid, and dimension 2 contains the real and imaginary parts. A shared CNN stem extracts local array-plane features at each (b, p, n) position and maps the input to

$$\mathbf{F}_0 = f_{\text{stem}}(\mathbf{X}_R), \quad \mathbf{F}_0 \in \mathbb{R}^{B \times P \times M_R \times C_e \times H \times V}. \quad (7)$$

Because the stem operates on the array plane, its parameters are independent of M_R .

ReFLEX uses the sample-level SNR as global side information. The condition encoder maps γ to a vector $\mathbf{z}_{\gamma} = \psi_{\gamma}([\gamma/20, 10^{-\gamma/20}]^T)$ via a small MLP, encoding the normalized dB SNR and the relative noise level; this vector is injected into the input features and Transformer blocks.

The backbone stacks D ReFLEX blocks, each applying frequency, polarization and spatial attention and a pointwise FFN. The reconstruction head predicts a correction $\Delta \mathbf{X}_R$, and the output is $\hat{\mathbf{X}}_R = \mathbf{X}_R + g(\mathbf{z}_{\gamma}) \Delta \mathbf{X}_R$, where g is an SNR-dependent gate; real and imaginary components are recombined into $\hat{\mathbf{H}}_R$.

B. Tensor-wise Axial Transformer Block

Instead of flattening CSI into a single token sequence, ReFLEX preserves the tensor

$$\mathbf{F} \in \mathbb{R}^{B \times P \times M_R \times C_e \times H \times V} \quad (8)$$

throughout the backbone. For each fixed (b, p, h, v) , frequency attention processes the observed-frequency sequence $\{\mathbf{F}_{b,p,n,:;h,v}\}_{n=1}^{M_R}$ and uses RFPB to represent relative frequency distance. For each fixed (b, n, h, v) , cross-polarization attention exchanges information between the two polarization components. For each fixed (b, p, n) , spatial attention operates on the HV array positions with a two-dimensional relative position bias.

With pre-normalization and residual connections, a block is written as

$$\mathbf{F}' = \mathbf{F} + \mathcal{A}_f(\text{Norm}(\mathbf{F}), \mathcal{S}_R), \quad (9)$$

$$\mathbf{F}'' = \mathbf{F}' + \mathcal{A}_p(\text{Norm}(\mathbf{F}')), \quad (10)$$

$$\mathbf{F}''' = \mathbf{F}'' + \mathcal{A}_s(\text{Norm}(\mathbf{F}''')), \quad (11)$$

$$\mathbf{F}_{\text{out}} = \mathbf{F}''' + \text{FFN}(\text{Norm}(\mathbf{F}''')), \quad (12)$$

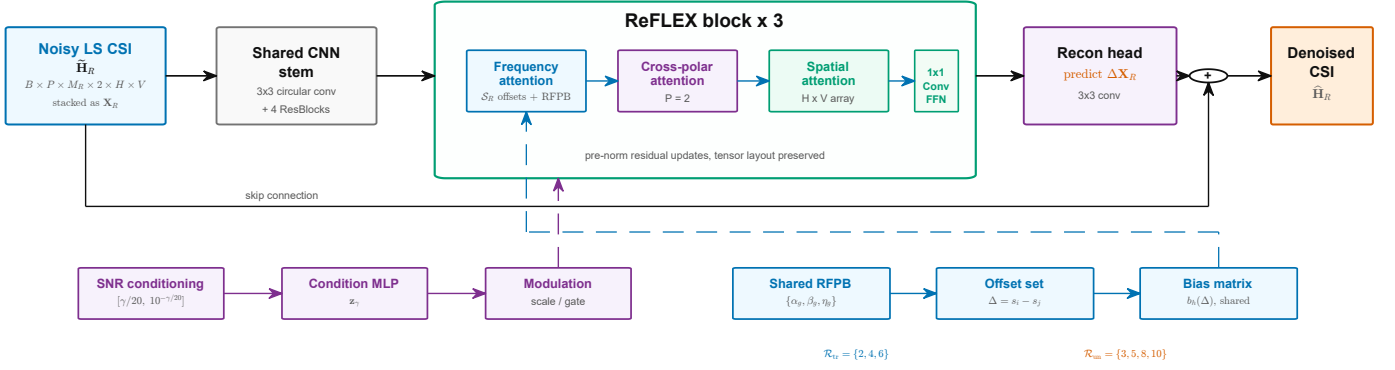


Fig. 1. Flowchart of ReFLEX. The CSI tensor structure is preserved while frequency, cross-polarization, and spatial axial attention are applied in each block. The shared RFPB is evaluated from the relative subcarrier offsets of the current observation set.

where \mathcal{A}_f , \mathcal{A}_p , and \mathcal{A}_s denote frequency, polarization, and spatial attention. Only \mathcal{A}_f depends on \mathcal{S}_R , and this dependence only determines the relative offsets used to generate the bias matrix.

C. Relative-Frequency Position Bias

RFPB is applied in frequency self-attention. For the h th attention head, the attention logit from observed subcarrier s_i to observed subcarrier s_j is

$$a_{ij}^{(h)} = \frac{(\mathbf{q}_i^{(h)})^T \mathbf{k}_j^{(h)}}{\sqrt{d_h}} + b_h(s_i - s_j), \quad (13)$$

where d_h is the per-head dimension, and the bias depends only on the relative subcarrier offset. Unlike absolute position encodings or fixed-length relative position tables [9], RFPB generates the bias from a continuous function of $\Delta = s_i - s_j$.

ReFLEX organizes frequency-attention heads into triplets. Because the subcarrier spacing is fixed at 30 kHz, the physical separation $\Delta f_{ij} = (s_i - s_j)\Delta f$ can be represented by Δ with a learnable scale. For the g th triplet, define

$$u_g(\Delta) = \alpha_g \Delta, \quad (14)$$

where α_g is a learnable frequency-scale parameter. The three bias curves are

$$b_{3g}(\Delta) = \eta_g \left(\frac{1}{1 + u_g^2(\Delta)} - \beta_g \right), \quad (15)$$

$$b_{3g+1}(\Delta) = \eta_g \frac{u_g(\Delta)}{1 + u_g^2(\Delta)}, \quad (16)$$

$$b_{3g+2}(\Delta) = -b_{3g+1}(\Delta), \quad (17)$$

where α_g , β_g , and η_g form a learnable triplet. In implementation, α_g uses a softplus parameterization to ensure nonnegativity, β_g uses a sigmoid parameterization and is constrained to $(0, 1)$, and η_g is a learnable scale. The first curve is even in Δ and favors nearby subcarriers, whereas the other two are odd and provide direction-sensitive offset features.

RFPB is motivated by OFDM frequency-domain correlation. Under the wide-sense stationary uncorrelated scattering assumption and an exponential power-delay profile, the

frequency-domain correlation is governed primarily by the subcarrier-index offset and can be written as

$$r_f[\kappa] = \frac{1}{1 + j2\pi\tau_{\text{rms}}\kappa\Delta f}, \quad (18)$$

where κ is the subcarrier-index offset, Δf is the subcarrier spacing, and τ_{rms} is the RMS delay spread. Its real part is even and decays with $|\kappa|$, and its imaginary part is odd. The RFPB triplet follows these symmetries as a structural prior rather than an estimate of the channel covariance.

Given a new observation set \mathcal{S}'_R , ReFLEX computes offsets $\Delta = s_i - s_j$ for $s_i, s_j \in \mathcal{S}'_R$ and uses the same $\{\alpha_g, \beta_g, \eta_g\}$ to generate the bias matrix, introducing no new RB-specific parameters.

IV. NUMERICAL RESULTS

A. Experimental Setup

Channels are generated by QuaDRiGa [10] using the 3GPP TR 38.901 UMa NLOS scenario [11]. The carrier frequency is 2.6 GHz, the subcarrier spacing is 30 kHz, and the base station uses an 8×8 dual-polarized antenna array. The RB train/test split follows Sec. II. Training SNRs are sampled uniformly from $[-20, 20]$ dB, and test SNRs are $-20 : 4 : 20$ dB. ReFLEX uses $D = 3$ axial Transformer blocks, embedding dimension 96, and 6, 2, and 6 heads for frequency, polarization, and spatial attention, respectively. The input stem contains one 3×3 circular convolution and 4 residual blocks with SNR conditioning. The batch size is 8, and the model is trained for 300 epochs.

For the NMSE experiments, the baselines are a CNN-style estimator based on the NVIDIA Aerial channel-estimation [12], frequency-only Practical LMMSE, and frequency-only Oracle-covariance LMMSE (Oracle-cov. LMMSE). Both LMMSE baselines are applied independently along subcarriers for each antenna/polarization port:

$$\mathbf{h}_{a,p,R} \in \mathbb{C}^{N_{\text{sc}}}, \quad \tilde{\mathbf{h}}_{a,p,R} = \mathbf{h}_{a,p,R} + \mathbf{e}_{a,p,R}. \quad (19)$$

Given covariance \mathbf{R}_f and noise variance σ^2 , the estimate is

$$\hat{\mathbf{h}}_{a,p,R} = \mathbf{R}_f (\mathbf{R}_f + \sigma^2 \mathbf{I})^{-1} \tilde{\mathbf{h}}_{a,p,R}. \quad (20)$$

Practical LMMSE constructs \mathbf{R}_f using the exponential-PDP correlation in (18), with τ_{rms} set to the channel-generation

RMS delay spread; it therefore assumes delay-spread side information but not sample covariance. Oracle-cov. LMMSE estimates \mathbf{R}_f from clean CSI samples drawn from the test distribution and assumes known σ^2 , making it a strong frequency-only linear reference rather than an absolute upper bound. These LMMSE references do not use spatial or polarization covariance.

The CNN baseline follows the default NVIDIA Aerial configuration with 32 convolutional channels. To avoid penalizing a fixed-length CNN for RB or SNR mismatch, an independent CNN is trained for each test RB/SNR pair and denoted by CNN-RB/SNR. This gives an oracle-style fixed-length neural reference that knows the target RB size and operating SNR but requires multiple specialized checkpoints.

Link-level performance is evaluated using multiuser NR PUSCH/UL-SCH simulations [8]. Channel estimation inputs are sparse LS estimates on the DM-RS time-frequency resource elements. The same ReFLEX checkpoint is applied per user at the observed DM-RS subcarrier positions, without retraining on sparse DM-RS patterns. The denoised sparse CSI is then linearly interpolated in time and frequency to the PUSCH resource grid used by the equalizer. The resulting CSI estimates are passed to the LMMSE equalizer for synchronous PUSCH data detection. The setup uses 12 single-layer UEs, 128 receive ports at the base station, and 1000 slots per SNR point. The PUSCH configuration uses mapping type B, DM-RS length 2, additional position 1, configuration type 2, and MCS index 10 (16QAM, target code rate 0.6426). To isolate CSI denoising, all methods share the same MCS, LDPC decoder, noise generation, equalizer, and receiver chain. The only changed component is the CSI estimate supplied to the equalizer.

B. NMSE on Unseen RB Lengths

Fig. 2(a) reports NMSE versus SNR on unseen RB lengths. ReFLEX gives lower NMSE than the considered baselines at low and moderate SNRs. At -20 dB, ReFLEX reaches -3.65 dB, whereas CNN-RB/SNR, Practical LMMSE, and Oracle-cov. LMMSE obtain -0.74 dB, -0.90 dB, and -1.38 dB, respectively. At 0 dB, ReFLEX reaches -15.23 dB, about 4.4 dB lower than CNN-RB/SNR and Practical LMMSE. At high SNR, Oracle-cov. LMMSE benefits from test-distribution covariance and known noise variance and approaches or exceeds ReFLEX near the highest SNRs. At 16 dB, ReFLEX obtains -24.83 dB and remains below CNN-RB/SNR and Practical LMMSE.

Fig. 2(b) shows average NMSE versus RB length. ReFLEX varies smoothly across seen RB2, RB4, and RB6 and unseen RB3, RB5, RB8, and RB10. The unseen-RB averages for RB3, RB5, RB8, and RB10 are -9.32 dB, -9.65 dB, -9.74 dB, and -9.75 dB, respectively. Although RB10 is longer than the maximum training length RB6, the NMSE does not degrade dramatically in this setup. CNN-RB/SNR and the LMMSE baselines yield higher average NMSE over the tested RB lengths.

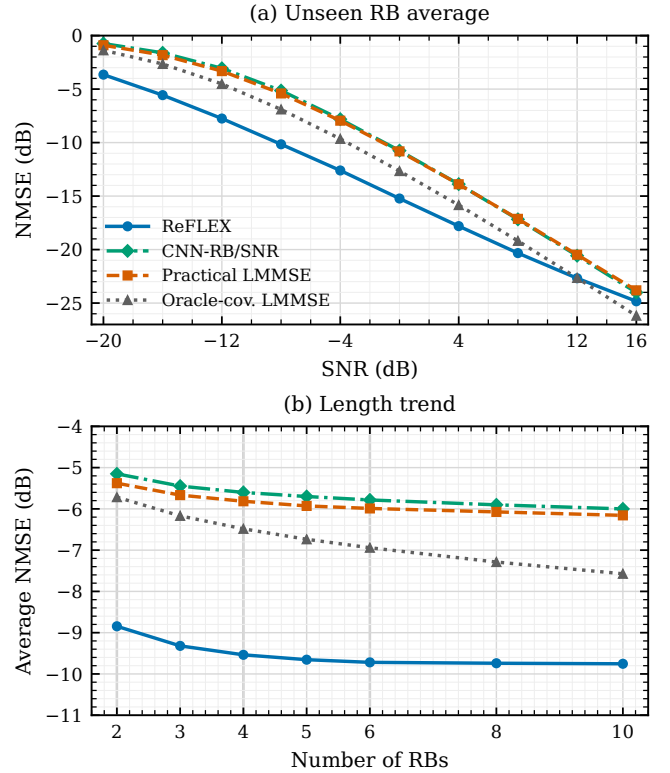


Fig. 2. NMSE comparison under the 3GPP 38.901 UMa NLOS scenario. The RB train/test split follows Sec. II. (a) Average NMSE-SNR curves on unseen RB lengths. (b) Average NMSE across RB lengths; gray vertical lines indicate training RBs.

C. Ablation and Checkpoint Analysis

Table I summarizes the average NMSE over the tested SNR values and RB lengths. ReFLEX achieves -9.61 dB on the unseen RB-length subset, compared with -5.76 dB for CNN-RB/SNR, -5.95 dB for Practical LMMSE, and -6.91 dB for Oracle-cov. LMMSE. Removing RFPB degrades the unseen-RB average to -7.47 dB and the RB10 average from -9.75 dB to -7.22 dB, which indicates that content-only attention is less stable for cross-length frequency modeling.

The absolute-position-encoding (absolute PE) ablation uses a fixed position table sized for RB10. Since the model is trained only on \mathcal{R}_{tr} , the position entries beyond RB6 are not directly supervised. Absolute PE reaches -9.46 dB on seen RB lengths, close to ReFLEX at -9.35 dB, but degrades to -8.24 dB on unseen RB lengths and to -6.84 dB on RB10. This behavior is consistent with absolute position indices tying the model to the training lengths. By contrast, ReFLEX trained only on RB4 still reaches -8.78 dB on unseen RB lengths and -8.25 dB on RB10, while multi-length training further improves performance.

CNN-RB/SNR requires one checkpoint per RB/SNR operating point. Therefore, a deployment covering N_R RB lengths and N_γ SNR levels requires $N_R N_\gamma$ CNN checkpoints. ReFLEX uses a single 1.646M-parameter checkpoint for all tested RB and SNR configurations.

TABLE I
ABLATION AND CHECKPOINT COMPARISON UNDER THE 3GPP 38.901
UMA NLOS SCENARIO.

Method	Train RB	Params	Seen avg.	Unseen avg.	RB10 avg.
Prac. LMMSE	–	–	–5.72	–5.95	–6.16
Oracle-cov. LMMSE	–	–	–6.35	–6.91	–7.57
CNN-RB/SNR	RB/SNR	$N_R N_\gamma \times 0.255M$	–5.50	–5.76	–6.00
ReFLEX	2,4,6	1.646M	–9.35	–9.61	–9.75
w/o RFPB	2,4,6	1.646M	–7.62	–7.47	–7.22
Absolute PE	2,4,6	1.657M	–9.46	–9.24	–6.84
RB4 only	4	1.646M	–8.75	–8.78	–8.25

NMSE is reported in dB; lower is better. Seen and unseen averages are computed over the RB subsets defined in Sec. II and over test SNRs $-20 : 4 : 20$ dB.

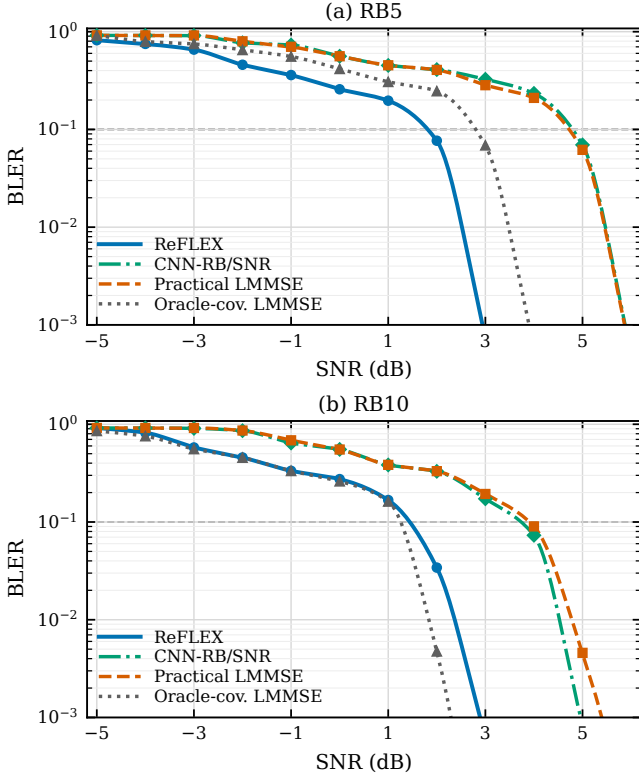


Fig. 3. NR PUSCH BLER on unseen RB lengths when the estimated CSI is used by a multiuser LMMSE equalizer. Markers are simulated points, and curves are shape-preserving guides in the log-BLER domain. (a) RB5. (b) RB10. The dashed line denotes 10% BLER; zero-error samples are omitted from the logarithmic axis.

D. Link-Level BLER

Fig. 3 reports coded-link performance on unseen RB5 and RB10 in the tested PUSCH setup. For RB5, ReFLEX reaches BLER 7.67×10^{-2} at 2 dB, whereas CNN-RB/SNR and Practical LMMSE yield 4.10×10^{-1} and 4.06×10^{-1} . The corresponding 10% BLER threshold is 1.72 dB, giving about 2.9 dB gains over CNN-RB/SNR and Practical LMMSE.

For RB10, ReFLEX achieves BLER 3.42×10^{-2} at 2 dB. The corresponding 10% BLER threshold is 1.32 dB, within 0.2 dB of Oracle-cov. LMMSE, and yields about 2.4 dB gains over CNN-RB/SNR and Practical LMMSE. Across RB5 and RB10, ReFLEX lowers the 10% threshold by about 2–3 dB relative to CNN-RB/SNR and Practical LMMSE.

V. CONCLUSION

This letter studied RB-length generalization for MIMO-OFDM CSI denoising under fixed subcarrier spacing. ReFLEX uses RFPB and axial attention to share one checkpoint across seen and unseen RB lengths. In the 3GPP TR 38.901 UMA NLOS setup, ReFLEX achieved about -9.6 dB average NMSE on unseen RB lengths and outperformed the Practical LMMSE and CNN-RB/SNR references. In NR PUSCH/UL-SCH link-level simulations on RB5/RB10, ReFLEX denoised sparse DM-RS LS estimates and reduced the 10% BLER threshold by 2–3 dB relative to these baselines. Future work includes other DM-RS patterns, larger RB allocations, and multi-scenario training.

REFERENCES

- [1] J.-J. van de Beek, O. Edfors, M. Sandell, S. K. Wilson, and P. O. Borjesson, "On channel estimation in OFDM systems," in *Proc. IEEE Veh. Technol. Conf. (VTC)*, vol. 2, Jul. 1995, pp. 815–819.
- [2] O. Edfors, M. Sandell, J.-J. van de Beek, S. K. Wilson, and P. O. Borjesson, "OFDM channel estimation by singular value decomposition," *IEEE Trans. Commun.*, vol. 46, no. 7, pp. 931–939, Jul. 1998.
- [3] H. Ye, G. Y. Li, and B.-H. Juang, "Power of deep learning for channel estimation and signal detection in OFDM systems," *IEEE Wireless Commun. Lett.*, vol. 7, no. 1, pp. 114–117, Feb. 2018.
- [4] D. Luan and J. S. Thompson, "Channelformer: Attention based neural solution for wireless channel estimation and effective online training," *IEEE Trans. Wireless Commun.*, vol. 22, no. 10, pp. 6562–6577, Oct. 2023.
- [5] L. Cheng, Z. Zhang, C. Dong, and S. Liu, "MSTGAN: A multi-slot conditional generative adversarial network based on Swin Transformer for channel estimation," *IEEE Commun. Lett.*, vol. 27, no. 7, pp. 1799–1803, Jul. 2023.
- [6] W. Zhou, Z. Zhang, Y. Yang, S. Yan, Z. Kong, and M. Debbah, "Diffusion inpainting MIMO-OFDM channels with limited noisy observations," arXiv:2604.09039, 2026.
- [7] D. Artemasov, A. Blagodarnyi, A. Sherstobitov, and V. Lyashev, "On autoregressive and neural methods for massive-MIMO channel denoising," *ITU J. Future Evol. Technol.*, vol. 5, no. 1, pp. 62–72, Mar. 2024, doi: 10.52953/MCKV3131.
- [8] 3GPP TS 38.211 v16.3.0, "NR; Physical channels and modulation," Tech. Spec., Oct. 2020.
- [9] P. Shaw, J. Uszkoreit, and A. Vaswani, "Self-attention with relative position representations," in *Proc. NAACL-HLT*, 2018, pp. 464–468.
- [10] S. Jaeckel, L. Raschkowski, K. Borner, and L. Thiele, "QuaDRiGa: A 3-D multi-cell channel model with time evolution for enabling virtual field trials," *IEEE Trans. Antennas Propag.*, vol. 62, no. 6, pp. 3242–3256, Jun. 2014.
- [11] 3GPP TR 38.901 v16.1.0, "Study on channel model for frequencies from 0.5 to 100 GHz," Tech. Rep., Jan. 2020.
- [12] NVIDIA, "Aerial CUDA-accelerated RAN channel-estimation notebook," online documentation. [Online]. Available: https://docs.nvidia.com/aerial/cuda-accelerated-ran/latest/content/notebooks/channel_estimation.html. Accessed: May 28, 2026.